Experimental verification of a gain reduction model for the space charge effect in a wire chamber

doi: 10.1093/ptep/ptx178

PTEP

Prog. Theor. Exp. Phys. **2018**, 013C01 (10 pages)
DOI: 10.1093/ptep/ptx178

Experimental verification of a gain reduction model for the space charge effect in a wire chamber

Naoki Nagakura[1,*], Kazuki Fujii[1], Isao Harayama[2], Yu Kato[1], Daiichiro Sekiba[2], Yumi Watahiki[2], and Satoru Yamashita[3]

[1]*Graduate School of Science, University of Tokyo, 7-3-1 Hongo, Bunkyo-ku, Tokyo 113-0033, Japan*
[2]*Graduate School of Pure and Applied Sciences, University of Tsukuba, 1-1-1 Tennodai, Tsukuba, Ibaraki 305-8577, Japan*
[3]*International Center for Elementary Particle Physics, University of Tokyo, 7-3-1 Hongo, Bunkyo-ku, Tokyo 113-0033, Japan*
*E-mail: nagakura@icepp.s.u-tokyo.ac.jp

Received September 15, 2017; Revised November 6, 2017; Accepted November 22, 2017; Published January 24, 2018

A wire chamber often suffers significant saturation of the multiplication factor when the electric field around its wires is strong. An analytical model of this effect has previously been proposed [Y. Arimoto et al., Nucl. Instrum. Meth. Phys. Res. A **799**, 187 (2015)], in which the saturation was described by the multiplication factor, energy deposit density per wire length, and one constant parameter. In order to confirm the validity of this model, a multi-wire drift chamber was developed and irradiated by a MeV-range proton beam at the University of Tsukuba. The saturation effect was compared for energy deposits ranging from 70 keV/cm to 180 keV/cm and multiplication factors 3×10^3 to 3×10^4. The chamber was rotated with respect to the proton beam in order to vary the space charge density around the wires. The energy deposit distribution corrected for the effect was consistent with the result of a Monte Carlo simulation, thus validating the proposed model.

Subject Index C30, H02, H11

1. Introduction

A wire chamber is a widely used detector in particle physics experiments. The output pulse height of its wires becomes degraded for the case of high multiplication factor or high beam flux [1]. This is caused by the reduction in electric field due to the large amount of ions existing around the anode wire, known as the space charge effect. The model to describe the gain reduction of a wire chamber due to the general space charge effect was established by R. W. Hendricks [2], and was experimentally verified using a high-flux X-ray beam. The numerical analysis of the gain reduction for a high-flux ion beam can be found in Refs. [3–5]. Regarding the self-induced space charge effect, although the gain reduction model was proposed in Ref. [6], no experimental study has been conducted to confirm its validity. This paper describes the experimental verification of such a model, in which a multi-wire drift chamber (MWDC) filled with He and CO_2 gas was irradiated by a proton beam from the Tandetron accelerator at the University of Tsukuba. The proton beam energy (E_p), the applied anode wire voltage (V_0), and the proton beam angle with respect to the anode wires of the MWDC

(ϕ) were changed. The dependence of the gain reduction on these parameters is compared with that predicted by the model.

2. Gain reduction model

This section introduces an analytical gain reduction model describing the space charge effect in Ref. [6]. Here, we assume a single-wire chamber with wire radius a and outer tube radius b in cylindrical coordinates, and a voltage V_0 applied to the wire. For simplicity, we assume that (i) the space charge distribution depends only on radius r, while being independent of ϕ and z, and (ii) the distribution remains unchanged during the avalanche process of all electrons. When a space charge of density $\rho(r)$ exists around the wire, the electric field for the nth electron can be expressed as

$$E_n(r) = \frac{V_0}{r\log(b/a)} - \frac{e}{2\pi\varepsilon a\Delta l}\left(\sum_{j=0}^{n-1} G_j\right)\left[\frac{1}{\log(b/a)}\int_a^b dr'\frac{\rho(r')}{r'} - \rho(r)\right], \tag{1}$$

$$E_n(r=a) = \frac{V_0}{a\log(b/a)} - \frac{eC}{2\pi a\varepsilon\Delta l}\left(\sum_{j=0}^{n-1} G_j\right), \tag{2}$$

where G_j is the multiplication factor for the jth electron, Δl is the length of wire around which space charge exists, and C is a constant describing the space charge effect. Assuming that the multiplication factor exponentially depends on the electric field, or $G_n = \exp(A + BE_n(r=a))$, the multiplication factor is expressed as

$$G_n = \frac{G_0}{1 + \dfrac{eBC}{2\pi\varepsilon a\Delta l}G_0}. \tag{3}$$

Using this formula, the gain reduction factor s, defined as the ratio of the multiplication factor to that without the space charge effect, can be expressed as

$$s \equiv \frac{1}{nG_0}\left(\sum_{j=0}^{n-1} G_j\right) \tag{4}$$

$$= \frac{\log\left(1 + \dfrac{eBC}{2\pi\varepsilon a\Delta l}nG_0\right)}{\dfrac{eBC}{2\pi\varepsilon a\Delta l}nG_0} \tag{5}$$

$$\equiv \frac{\log\left(1 + fG_0\dfrac{dE}{dl}\right)}{fG_0\dfrac{dE}{dl}}, \tag{6}$$

where $w \equiv dE/n$ is the average energy loss per electron–ion pair creation by incident charged particle (w-value). G_0 represents the multiplication factor without space charge, which can be determined by energy calibration. $f \equiv eBC/2\pi\varepsilon aw$ is a constant including all microscopic characteristics of the space charge effect, which determines the absolute scale of gain reduction. Since it is hard to calculate analytically, f is treated here as a fitting parameter. Equation (6) monotonically decreases with dE/dl and G_0, and is shown in Fig. 1 for three values of f.

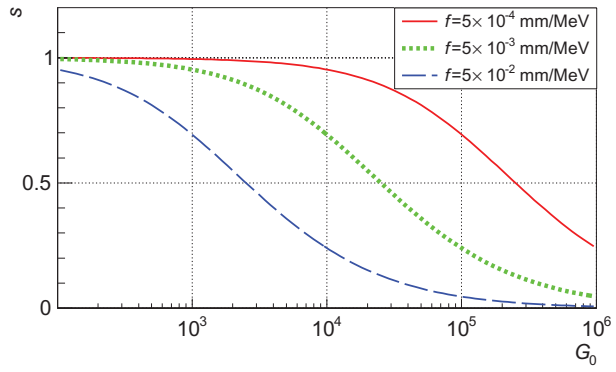

Fig. 1. Gain reduction factor (s) calculated by the gain reduction model in Eq. (6) as a function of the multiplication factor (G_0). The function is shown with three values of f. Here, dE/dl is fixed at the typical value of 20 keV/mm.

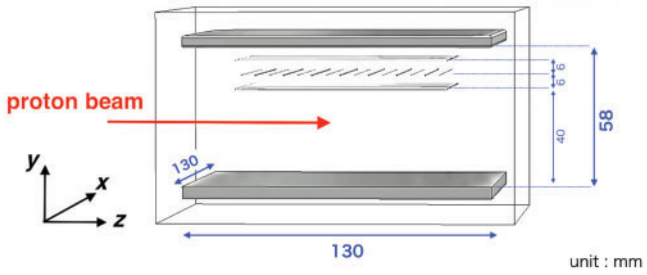

Fig. 2. The schematic layout of the MWDC. The sensitive region is defined by two electrode plates. The multi-wire region comprises 8 anode wires, 7 field wires, and 30 cathode wires.

3. Experimental setup

This section describes the detailed experimental setup to measure the gain reduction introduced in Sect. 1.

3.1. Multi-wire drift chamber

Figure 2 shows the overall structure of the MWDC, which has dimensions of 13 cm × 13 cm × 6 cm. It is made of G10 FR-4, or glass–epoxy laminate, and housed in a 14 L vacuum chamber filled with 85 kPa He gas and 15 kPa CO_2 gas. Electrons are drifted by an electric field of 4×10^2 V/cm in the y-direction, towards the multi-wire region located in the upper part of the MWDC. One layer of wires is made of 8 anode wires and 7 field wires, while each of the other two layers is made of 15 cathode wires. The anode and field wires are arranged alternatively in the x-direction, which is orthogonal to the cathode wires arranged in the z-direction in the planes above and below the anode- and field-wire plane (see Fig. 3).

In standard operation, $V_0 = 1700$ V is applied to the anode wires, which corresponds to a multiplication factor of about 10^4. The detailed parameters of the MWDC are listed in Table 1, and its performance is given in Sect. 4.

3.2. Tandetron accelerator and vacuum chamber

The MWDC was irradiated by the MeV-range proton beam at the beamline of the 1 MV Tandetron accelerator at UTTAC (University of Tsukuba, Tandem Accelerator Complex). The Tandetron accelerator performs a two-step acceleration with a single voltage by converting an electric charge of negatively charged ions on a positive high-voltage terminal. Figure 4 shows a schematic view of

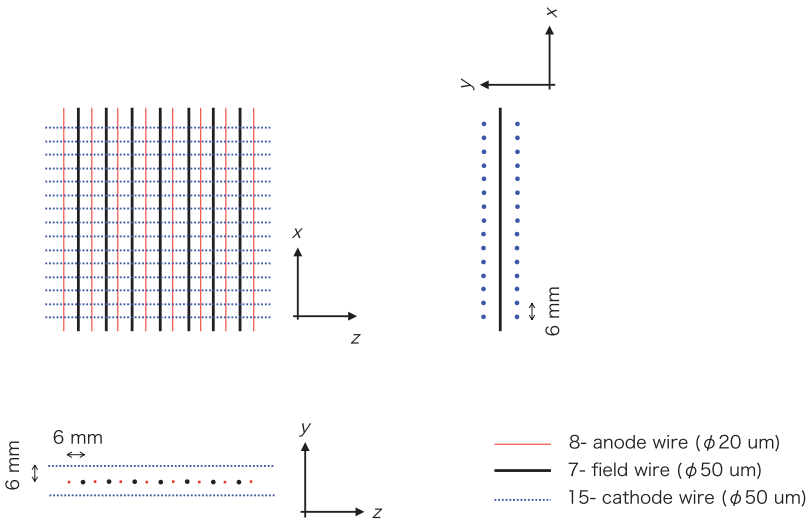

Fig. 3. Wire geometry of the MWDC.

Table 1. MWDC specification.

overall size	130 mm (x) ×58 mm (y) × 130 mm (z)
sensitive region	90 mm (x) × 40 mm (y) × 90 mm (z)
rotation range	40°–90° (w.r.t. beam direction)
gas composition	He: 85 kPa, CO_2: 15 kPa
drift field strength	4×10^2 V/cm
anode wire (8 ch)	Au/W, 20 μm diameter
field wire (7 ch)	Au/W, 50 μm diameter
cathode wire (15 × 2 ch)	Au/W, 50 μm diameter
wire pitch	6 mm
multiplication factor	$\sim 10^4$
anode voltage (V_0)	$\sim$ 1700 V
upper electrode voltage	0 V
lower electrode voltage	−1500 V

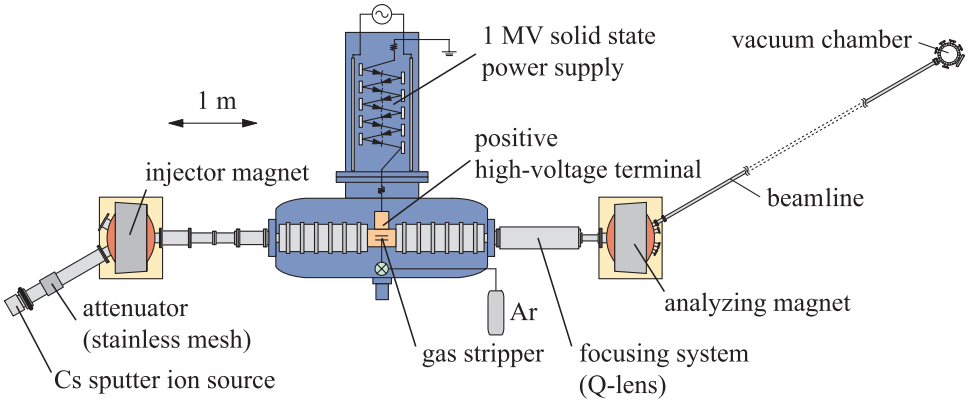

Fig. 4. Overview of the 1 MV Tandetron accelerator at the University of Tsukuba.

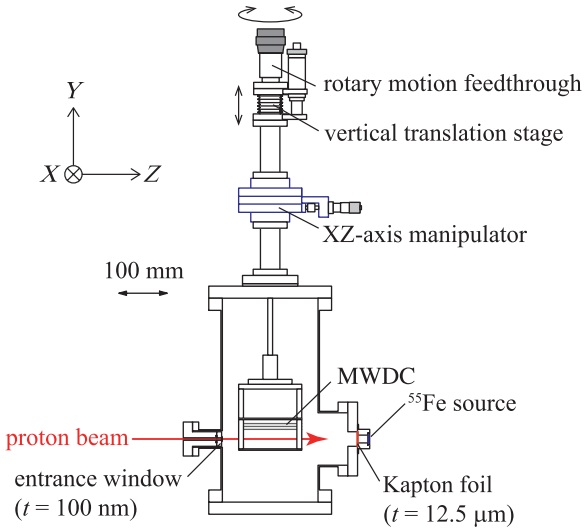

Fig. 5. A schematic view of the vacuum chamber with the MWDC.

the accelerator and the beamline. Hydrides (H^-) were generated from a pressed TiH_2 solid cathode in the Cs sputter ion source. The beam current can be attenuated by a stainless mesh existing at the downstream side of the ion source. The protons were produced after converting the electric charge with an Ar-based stripper (gas stripper) in the terminal. The obtained proton beam can be accelerated up to 2 MeV by the Tandetron accelerator, and only protons with a specified energy can be guided to the beamline by a magnet. After passing through the analyzing magnet, the proton beam was shaped into a size of 1×1 mm^2 by both a slit system and the entrance window of the vacuum chamber housing the MWDC. In this setup, the beam divergence and the flux were limited to about 1 mrad and 10 cps, respectively. The vacuum chamber with the MWDC was connected to the downstream side of the beamline at the Tandetron accelerator [7].

Figure 5 shows a schematic drawing of the vacuum chamber. The MWDC can be rotated by a rotary motion feedthrough in the plane parallel to its wires, which allows variation of the energy deposit density per anode wire length (dE/dl). The entrance window is made of a 100 nm Si_3N_4 plate from Silson Ltd (Northampton, UK), which separates the gas volume in the vacuum chamber and the high vacuum zone in the beamline while maintaining the energy loss of the proton beam below 1%.

3.3. Energy calibration system

The energy calibration of the MWDC was conducted using a ^{55}Fe source, which emits monochromatic K_α X-rays of 5.9 keV. The X-rays were collimated only in the y-direction, while being able to reach the entire effective region of the MWDC in the x–z plane. The X-rays were injected into the gas volume through a 50 mm $\times$ 29 mm Kapton foil with a thickness of 12.5 μm. The position of the MWDC is variable in the y-direction with respect to the source, which enables the acquisition of the energy calibration data with different electron drift lengths. The capturing process of electrons during their drift can be corrected using these results.

3.4. Data acquisition system

The schematics of the data acquisition system for the MWDC is shown in Fig. 6. The waveforms of 8 anode wires, 7 field wires, and 15 cathode wires in the lower plane were digitized using the front-end

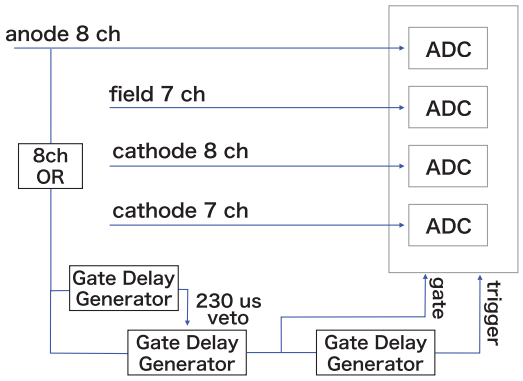

Fig. 6. The schematics of the data acquisition system.

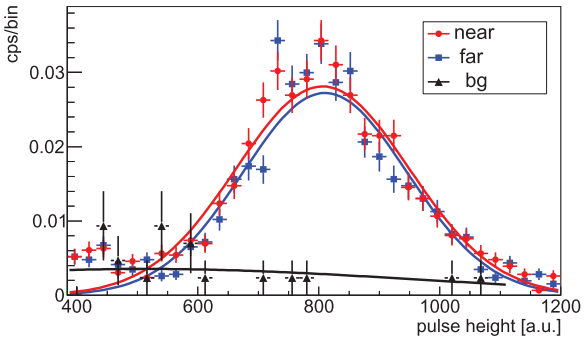

Fig. 7. Pulse height distribution for the ^{55}Fe X-ray with its electron drift length of 1 cm (red) and 3 cm (blue), respectively. The background distribution is also shown (black).

instrumentation entity for sub-detector specific electronics (FINESSE). The FINESSE module can be operated in the Copper-Lite system [8]. The trigger signal for recording these waveforms was produced if any of the total 8 anode wires exceeded the threshold voltage of 50 mV. Each waveform was digitized by a 12-bit ADC with a sampling rate of 25 MHz. The charge signal induced at each wire was amplified by a charge-sensitive preamplifier installed at the top of the MWDC. The amplification gain of the preamplifier was set to be 1.3 V/pC for ^{55}Fe X-ray events, and 0.54 V/pC or 0.094 V/pC for proton events, respectively.

4. Detector performance

In this section, the performance of the developed MWDC is introduced in detail.

4.1. Response to monochromatic X-ray

Figure 7 shows the pulse height distribution for ^{55}Fe X-rays combining 4 center anode wires. Here, the clearly visible pulse height peaks correspond to photoabsorption events for 5.9 keV X-rays. The red and blue histograms represent the distributions of different drift lengths of 1 cm and 3 cm, respectively. The corresponding energy resolution, defined as sigma over mean, is 13.2% and 14.5%, respectively. The attenuation length of the drift electron is estimated to be 20 cm even in the worst case; this was monitored and corrected during the proton measurement. The distribution without the source is also shown in Fig. 7 in black.

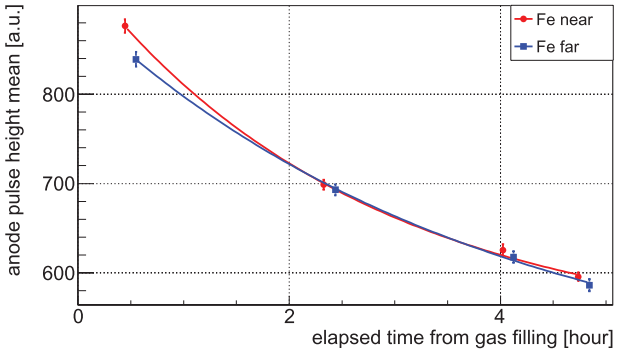

Fig. 8. The variation of the peak position for the ^{55} Fe X-ray over an extensive period of time. The drift length of the electrons is set at 1 cm (red) and 3 cm (blue).

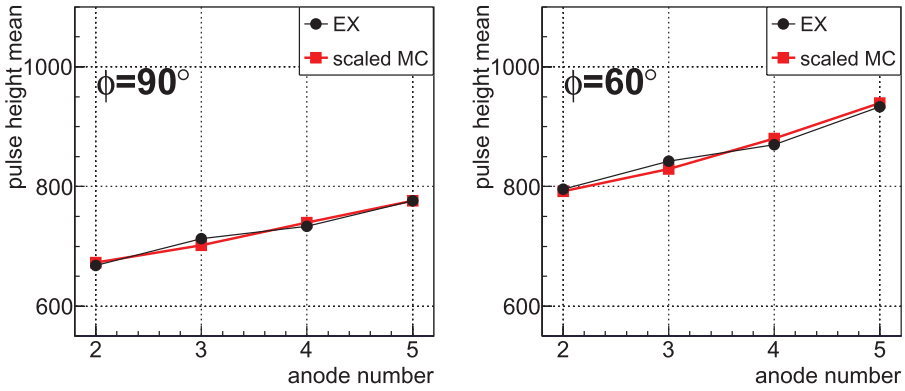

Fig. 9. Comparison of the anode pulse height from experiment (black) and the energy deposit calculated by the Monte Carlo simulation (red) for $E_p = 2.00$ MeV. ϕ was set between 40° to 90°, and $V_0 = 1350$ V was applied. Here, the distribution of the calculated energy deposit was normalized so that its integral is in accordance with that of the experimental distribution.

4.2. Stability

The long-period data of the MWDC were taken in order to evaluate the effects of gas contamination and charge accumulation. The transition of the ^{55}Fe X-ray peak position is shown in Fig. 8, where red and blue represent drift lengths of 1 cm and 3 cm, respectively. The decrease in the pulse height was measured to be about 5–10% per hour, which was described by an exponential function. Thus ^{55}Fe X-ray data were taken before, after, and in the middle of the proton measurement to interpolate the calibration factor by an exponential function.

5. Results

5.1. Energy deposit distribution at low anode voltage

The output pulse height for the proton beam was initially measured at a multiplication factor of about 10^3. This result was compared with the energy deposit calculated by the Geant4-based Monte Carlo simulation [9] with the MWDC geometry. E_p was set at 1.35 MeV, 1.68 MeV, and 2.00 MeV, and V_0 at 1350 V, 1310 V, 1250 V, respectively. ϕ was changed at intervals of 10° between 40° to 90° for every measurement condition. The energy deposit in the TPC sensitive region is calculated to be 70 keV/cm to 80 keV/cm for a 2.00 MeV proton beam and 140 keV/cm to 190 keV/cm for a 1.35 MeV proton beam, respectively. Figure 9 shows a comparison between the pulse height distribution and calculated energy deposit at $E_p = 2.00$ MeV. This energy was sufficient for the

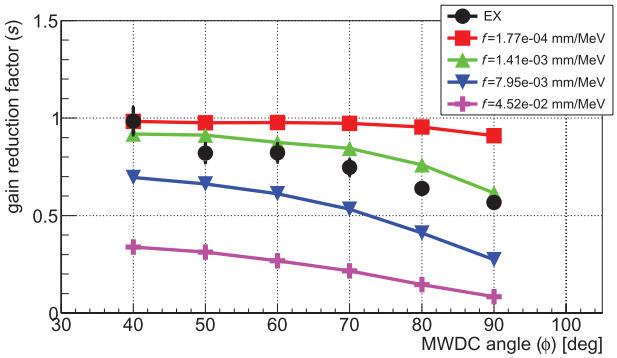

Fig. 10. Result of s for the proton beam measured at anode wire 4 as a function of ϕ at $E_p = 2.00$ MeV and $V_0 = 1700$ V.

proton beam to pass through the sensitive region of the MWDC from anode wire 0 to anode wire 7. The calculated distribution of the energy deposit was normalized in this plot so that its integral is in accordance with that of the experimental distribution. The energy deposit distribution of the anode wires was reproduced by the energy deposit calculated using the Monte Carlo simulation. The experimental distribution of different beam energies was similarly reproduced by the Monte Carlo simulation.

5.2. *Gain reduction factor at high anode voltage*

Next the pulse height for the proton beam obtained with a relatively high multiplication factor (about 10^4) was compared with the energy deposit calculated by the Monte Carlo simulation. V_0 was set at 1540 V, 1570 V, 1700 V, and 1775 V for $E_p = 2.00$ MeV, and 1510 V, 1700 V, and 1760 V for $E_p = 1.35$ MeV. The multiplication factor corresponds to about 3×10^3 for $V_0 = 1540$, and 2×10^4 for $V_0 = 1760$. The data were taken by changing ϕ at intervals of 10° between 40° to 90° to find the dependence on dE/dl.

In this measurement, s was derived as the ratio of the output pulse height to the calculated energy deposit. ^{55}Fe X-ray data were taken in between the proton measurements for energy calibration and to correct for the attenuation effect of the electrons. Figure 10 shows the obtained s distribution of anode wire 4 at $V_0 = 1700$ V and $E_p = 2.00$ MeV. The results of the Monte Carlo simulation for different input values of f are also shown in the figure. The decrease of s with respect to ϕ can be described by the increase of dE/dl.

5.3. *Comparison of the result with the Monte Carlo simulation*

The value of s was calculated based on the Geant4-based Monte Carlo simulation with the gain reduction model described in Sect. 2. The value was compared with the experimental result, and the f value that minimizes χ^2/ndf was selected as the optimum value. Figure 11 shows the overall result of the derived f values combined with different values of E_p and V_0. The f values are consistent with each other within their respective uncertainties, and averaged at $\overline{f} = (1.8^{+0.5}_{-0.4}) \times 10^{-3}$ mm/MeV. The experimental result of s as a function of ϕ was compared with the gain reduction model assuming this parameter, as shown in Fig. 12. The comparison of the energy deposit distribution before and after correcting for the space charge effect is also shown in Fig. 13, along with the energy deposit distribution calculated by the Monte Carlo simulation. The energy deposit distribution corrected for the space charge effect using the proposed model was able to reproduce the result of the Monte Carlo simulation, showing the validity of the model.

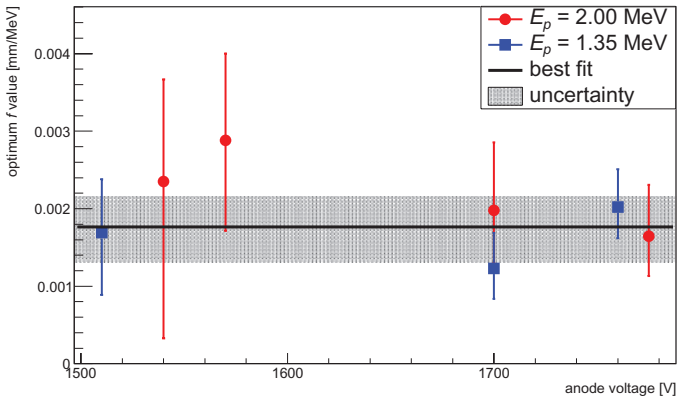

Fig. 11. Combined result of the optimum f values. The black line represents the averaged value $\overline{f} = (1.8^{+0.5}_{-0.4}) \times 10^{-3}$ mm/MeV.

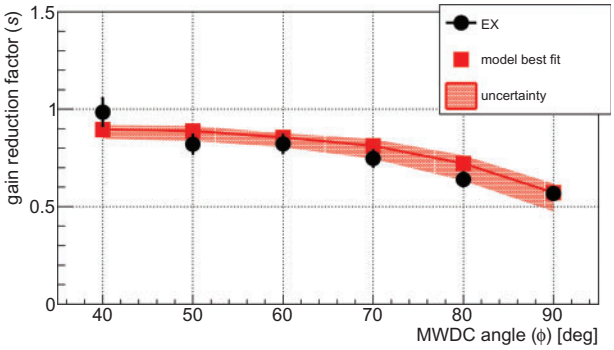

Fig. 12. Comparison of the measured gain reduction factor and the gain reduction model including the f uncertainty.

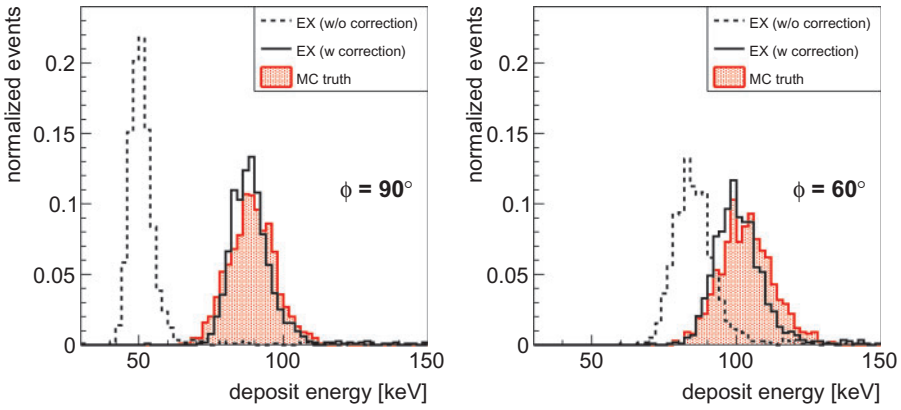

Fig. 13. Comparison of the enegy deposit distribution without and including the correction for the gain reduction model. The distribution is obtained at anode wire 4, $E_p = 2.00$ MeV, and $V_0 = 1700$ V.

6. Conclusion

An analytical model was developed for the gain reduction of a wire chamber caused by space charge existing around its wires. This model describes the gain reduction as a function of dE/dl, G_0, and one constant parameter. In order to confirm the validity of the model, an MWDC was developed and irradiated by a proton beam from a Tandetron accelerator. E_p, V_0, and ϕ were varied during the measurement. The value of the constant parameter was determined for various combinations of E_p

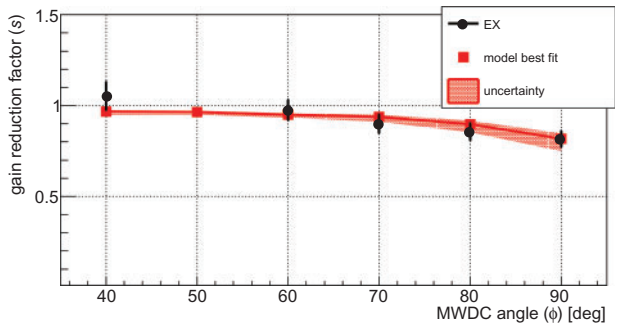

Fig. A1. Result of s for the proton beam measured at anode wire 4 as a function of ϕ at $E_p = 2.00$ MeV and $V_0 = 1540$ V.

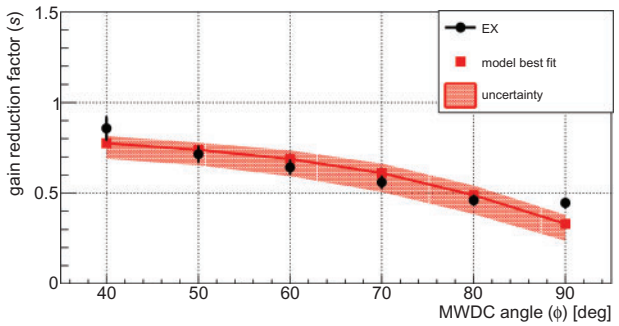

Fig. A2. Result of s for the proton beam measured at anode wire 2 as a function of ϕ at $E_p = 1.35$ MeV and $V_0 = 1760$ V.

and V_0 by comparing the gain reduction with Monte Carlo simulation. The obtained values were consistent with each other within their respective uncertainties. Using its average, the observed pulse height distribution was able to reproduce the distribution of the Monte Carlo simulation. Thus the validity of the gain reduction model was confirmed.

Acknowledgements

This work was supported by JSPS KAKENHI Grant Numbers JP16J01507, JP16H02194. The experiment at the University of Tsukuba was supported by the JST CUPAL program.

Appendix. Gain reduction factor for different beam energies and anode wire voltages

Results of the gain reduction factor (s) for different beam energies and anode wire voltages are shown in Figs. A1 and A2.

References

[1] S. Koperny and T. Z. Kowalski, Nucl. Phys. B Proc. Suppl. **197**, 370 (2009).
[2] R. W. Hendricks, Rev. Sci. Instrum. **40**, 1216 (1969).
[3] W. Riegler, C. Lippmann, and B. Schnizer, Nucl. Instrum. Meth. Phys. Res. A **582**, 469 (2007).
[4] K. Katagiri, T. Furukawa, E. Takeshita, and K. Noda, J. Plasma Fusion Res. SERIES **9**, 614 (2010).
[5] K. Katagiri, T. Furukawa, E. Takeshita, and K. Noda, Proc. IPAC'10, MOPD102, p. 942 (2010).
[6] Y. Arimoto et al., Nucl. Instrum. Meth. Phys. Res. A **799**, 187 (2015).
[7] D. Sekiba, K. Chito, I. Harayama, Y. Watahiki, S. Ishii, and K. Ozeki, Nucl. Instrum. Meth. Phys. Res. B **401**, 29 (2017).
[8] Y. Igarashi et al., IEEE Trans. Nucl. Sci. **52**, 2866 (2005).
[9] S. Agostinelli et al., Nucl. Instrum. Meth. Phys. Res. A **506**, 250 (2003).